Climatology of gravity waves–induced electric fields in the equatorial *E* region

H. C. Aveiro,[1] C. M. Denardini,[1] and M. A. Abdu[1]

Received 25 February 2009; revised 13 June 2009; accepted 17 July 2009; published 14 November 2009.

[1] Equatorial electrojet (EEJ) observations using VHF radars show backscattered echoes from two types of electron density irregularities explained by the modified two-stream (Type I) and the gradient drift (Type II) instabilities. From the Type II irregularity velocities obtained by a radar installed at São Luiz Space Observatory (2.58°S, 44.23°W, magnetic latitude 0.23°S) we have inferred the vertical electric fields (E_z). The E_z inference was based on geomagnetic field and atmospheric models. A harmonic analysis of these electric fields shows the presence of gravity waves (GW) induced oscillations in the EEJ. We calculated the ratio between GW-related electric fields and the total E_z, which is an indicator of the efficiency in the production of an additional electric field due to a gravity wave neutral wind. In the present paper we describe the methodology of analysis and discuss some characteristics of the gravity waves that could modify the equatorial ionospheric electric fields.

Citation: Aveiro, H. C., C. M. Denardini, and M. A. Abdu (2009), Climatology of gravity waves–induced electric fields in the equatorial *E* region, *J. Geophys. Res.*, *114*, A11308, doi:10.1029/2009JA014177.

1. Introduction

[2] At about 105 km of altitude in the equatorial *E* region and covering a latitudinal range of ±3° around the dip equator flows an intense electric current named equatorial electrojet (EEJ) [*Forbes*, 1981] and driven by the *E* region dynamo [*Fejer and Kelley*, 1980]. Studies of the equatorial ionosphere using VHF radars have shown echoes backscattered from plasma irregularities in the EEJ. Spectral studies of such echoes showed two distinct signatures for the observed irregularities, that were labeled Type I and Type II. They are also known for their theory of development as modified two-stream [*Farley*, 1963; *Buneman*, 1963] and gradient drift instabilities [*Rogister and D'Angelo*, 1970], respectively. Type II echoes show a broader spectrum with smaller amplitude than the Type I echoes. Type I irregularities travels closely to the ion-acoustic speed, while Type II irregularity phase velocity (V_{pII}), as measured by radar, is given by [*Broche et al.*, 1978]:

$$V_{pII} = \left(V_{pII}\right)_0 + \frac{\mathbf{k}}{k}\cdot\mathbf{V_n} + \frac{\mathbf{k}}{k}\cdot\frac{\langle\mathbf{V_n}\rangle - \mathbf{V_n}}{1+\psi} \qquad (1)$$

where $(V_{pII})_0$ is the phase velocity that would be observed if the wind were absent, $\mathbf{k}$ is the wave vector of the irregularity motion, V_n is the neutral wind velocity at the point of interest, $\langle V_n\rangle$ is its value averaged along the whole magnetic field line, and $\psi = (\nu_i \cdot \nu_e)/(\Omega_i \cdot \Omega_e)$, where $\Omega_{e,i}$ is the gyrofrequency and $\nu_{e,i}$ is the collision frequency. The subscripts e and i indicate the electron and ion terms, respectively. Assuming that $\mathbf{V_n} = \langle\mathbf{V_n}\rangle$, we remain just with the first two terms in equation (1). This condition is fulfilled if the curvature of Earth's magnetic field is neglected (they are horizontal) and if the winds depend only on the altitude [*Broche et al.*, 1978], which should correspond to the results of *Sato* [1975].

[3] Gravity wave represents a source of dynamical fluctuations in the electrojet region [*Forbes*, 1981]. *Reddy and Devasia* [1976] reported short-period (20–30 min) fluctuations in the electron drifts ($\delta V_D \sim 25$–50 m/s) in their VHF radar measurements at Thumba correlated with horizontal magnetic variations at Trivandrum. *Anandarao et al.* [1978] inferred vertical winds of the order of 10–20 m/s with a vertical wavelength of 50 km from analysis of a barium cloud release over Thumba, which they interpreted as being of gravity wave origin. The generation of electric fields by gravity wave winds in the equatorial ionosphere was investigated by *Kato* [1973] using a one-dimensional (vertical) analysis, which was later modified in a two-dimensional treatment by *Anandarao et al.* [1977].

[4] In the present paper, we analyze the signatures of the presence of gravity waves–induced electric fields in the EEJ through spectral analysis and statistics. We summarize some characteristics of these GW's and discuss the methodology of analysis. Since the origin of ionospheric zonal electric fields may also be credited to magnetospheric sources [*Earle and Kelley*, 1987], our data set is composed only with radar data in magnetically quiet days.

2. Experiment and Data Analysis Technique

[5] For such study we have used the RESCO radar located at São Luís, Brazil [*Abdu et al.*, 2002; *Denardini*

[1]Divisao de Aeronomia, Instituto Nacional de Pesquisas Espaciais, Sao Paulo, Brazil.

0148-0227/09/2009JA014177

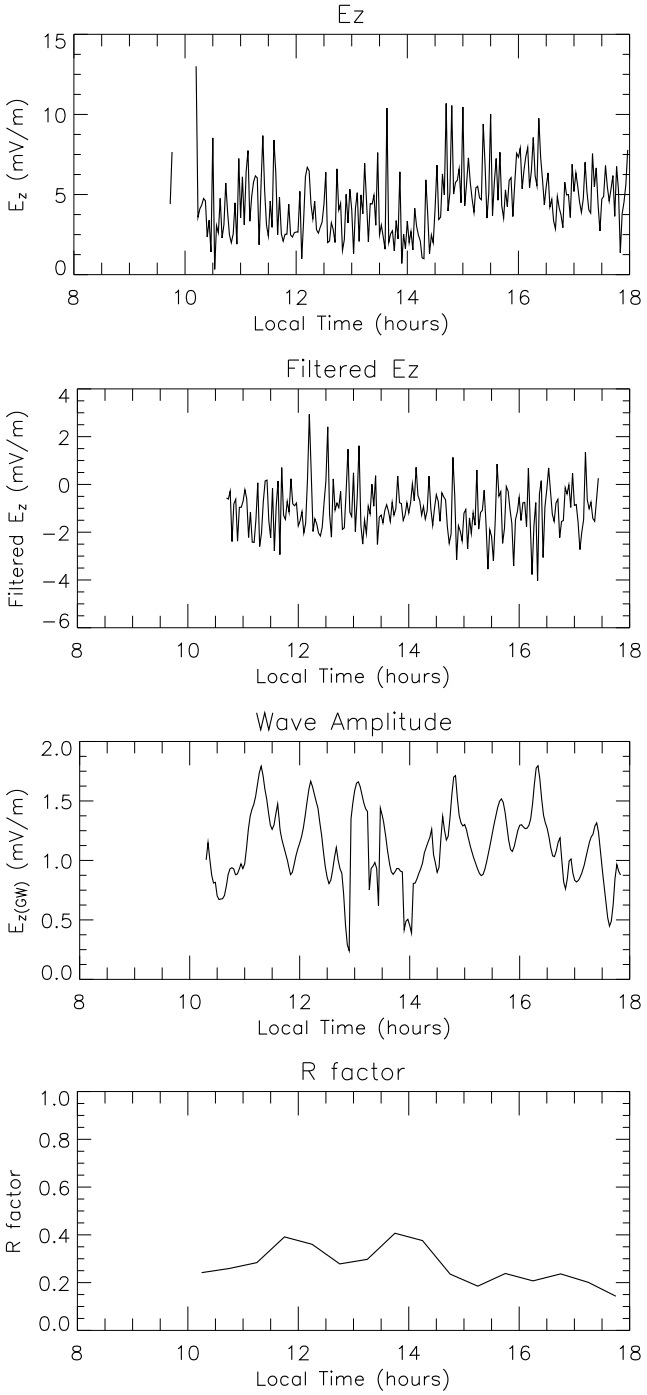

Figure 1. Height median of the vertical electric field, filtered field, filtered wave amplitude, and efficiency factor for 6 February 2001.

et al., 2004], for EEJ soundings. The interpulse period (IPP) of transmission is usually set to 1 ms. The time delay (TD) between transmission and acquisition is set to 620 μs, which corresponds to the minimum height sampled to be 80.5 km. The observations have been made using a pulse width (PW) of 20 μs that corresponds to 3 km height resolution using the vertical beam or 2.6 km when the radar beam is oblique. The radar data acquisition system samples the echoes so that the height coverage is between around 80 and 120 km, divided in 16 range gate samples, that are stored in a sequential binary file. The signals are grouped in sets corresponding to 256 pulses (NP) for each sampled range gate. The data processing consisted in an off-line spectral analysis using Fast Fourier Transform (FFT) for each range gate of NP data points which resulted in the spectral distribution of the Doppler frequencies contained in the returned signal for each range gate. For the periods of analysis, the time resolution between each set of NP pulses is 12 s and the aliasing frequency for each spectrum is 500 Hz with $\sim$4 Hz (NP = 256) of frequency resolution.

[6] The Doppler spectrum of the echoes is a composite of both Type I and Type II irregularities present inside the volume sampled by the radar. Therefore, the Gaussian fit technique was applied to each spectrum. Thus, each Gaussian (related to one specific irregularity type) is characterized by three parameters: center of frequency distribution (corresponding to Doppler shift), spectral power density, and spectral width. After inverting the curves, the six statistical moments (three to each irregularity type) are evaluated. Fitted curves with spectral power smaller than 5% of the maximum spectral power for the whole day are discarded to avoid eventual bad fitting related problems. Finally, the phase velocity estimates for Type II irregularities (V_{pII}, in m/s), which were obtained by the fitting procedure, are used to calculate the vertical electric field (E_z), as given by:

$$E_z = \frac{V_{pII}}{\sin\phi} \cdot (1 + \psi) \cdot \frac{B^2}{H}, \tag{2}$$

where ϕ is the beam zenith angle (30° eastward), H is the horizontal component of the magnetic flux density **B**, and B is defined as $|\mathbf{B}|$. For a more complete explanation about the E_z computation, see *Aveiro et al.* [2009].

3. Results

3.1. Efficiency of GW-Induced Electric Fields

[7] The analysis was performed using data collected from the eastward looking radar beam during some magnetically quiet days (Kp $\leq$ 3+) in 2001, 2002, and 2004. Disturbed days were discarded so that amplitude oscillations in electric fields would be mainly caused by atmospheric waves. The steps to calculate the GW-induced electric fields efficiency (R_{GW}) factor using wavelet transform are: (1) apply Continuous Wavelet Transform (CWT) using the wavelet mother of Morlet to vertical electric fields; (2) reconstruct the electric fields over scales in the range from 4- to 30-min (short-period gravity waves); and (3) calculate the ratio between the reconstructed (sinusoidal waves) electric field and the total electric field (original time series), i.e., the estimated R_{GW} factor.

[8] The analysis was constrained to the 100–110 km heights, where the backscatter EEJ power is stronger. Based on the RESCO radar parameters applied to the EEJ sounding, it resulted in a vertical electric field with 3 points in height and 2-min resolution. The height median of the vertical electric field, filtered field, filtered wave amplitude, and efficiency factor is calculated. An example of these parameters for 6 February 2001 is shown in Figure 1.

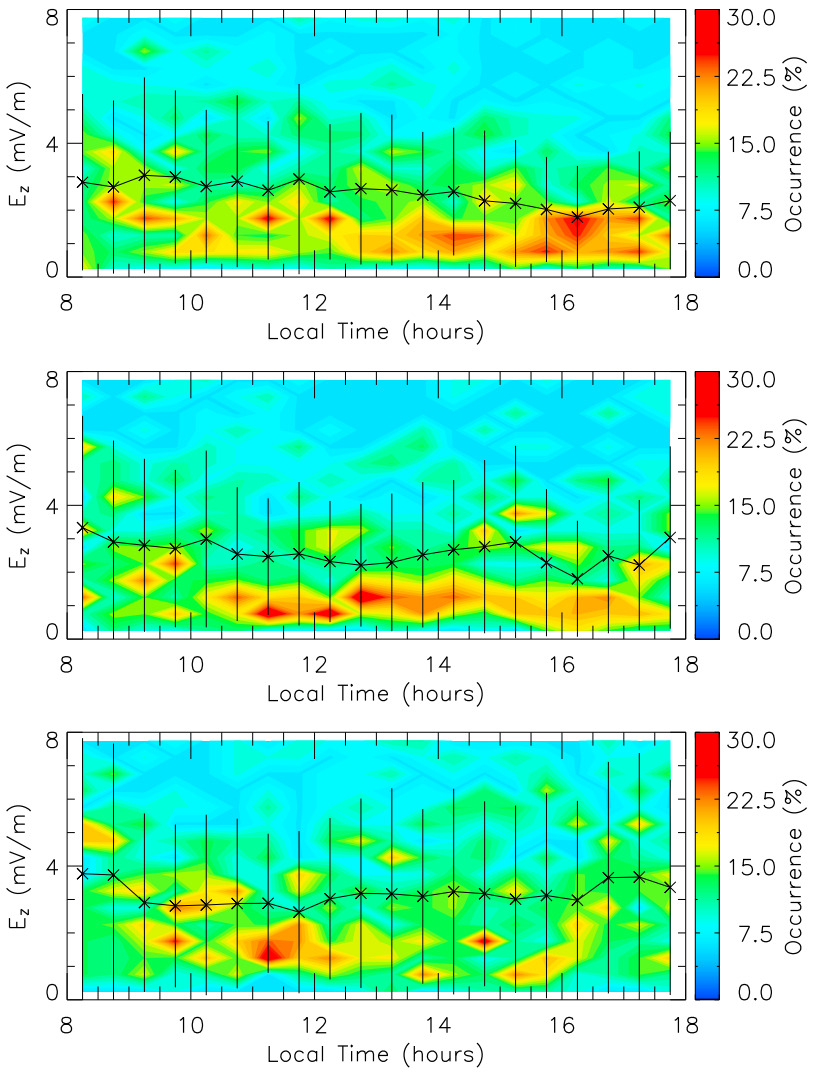

Figure 2. Statistics of occurrences of E_z amplitude as function of time for (top) solstice D months, (middle) equinoctial E months, and (bottom) solstice J months. The continuous line represents the average vertical electric field for each 30-min interval, and the vertical line is the standard deviation of E_z.

[9] Further, to examine the seasonal variation of the R_{GW} factor, the data were grouped into the following Lloyd season classification [*Eleman*, 1973]: (1) D months consisting of November, December, January, and February representing local summer season; (2) E months consisting of March, April, September, and October; and (3) J months consisting of May, June, July, and August months representing local winter season. We have selected 51 days on J months, 50 from E months, and 79 on D months.

[10] Figure 2 shows the statistics of vertical electric field (E_z) binned in 30-min intervals and 0.5 mV/m for solstice D months (Figure 2, top), equinoctial E months (Figure 2, middle), and solstice J months (Figure 2, bottom). The occurrence percentage at any E_z value is calculated with reference to the total number of the occurrences of all observed E_z values at any local time (LT), so that the sum of each vertical line gives 100% of occurrence. The continuous line represents the average vertical electric field for each 30-min interval and the vertical bar is the standard deviation of E_z. The results show that the average vertical electric fields in D months in general does not exceed 3 mV/m, though the standard deviation indicates E_z of up to 6 mV/m. The average E_z varies from 3 mV/m (at 8 LT) to 2 mV/m (at 18 LT). The average vertical electric field for both E and J seasons shows a variation from around 4 mV/m to 3 mV/m. So, it seems that the vertical electric fields are weaker in local summer (D) months. In general, E_z in J months is stronger than in the others. The standard deviation shows also that the vertical electric fields present a major variability in local winter (J) months than in other seasons.

[11] The vertical electric field perturbations produced by gravity wave winds ($E_{z(GW)}$) is obtained as described before. The statistics of $E_{z(GW)}$ amplitude as function of time for solstice D months (Figure 3, top), equinoctial E months (Figure 3, middle), and solstice J months (Figure 3, bottom), is shown in Figure 3. The vertical and horizontal lines have the same meaning as in Figure 2, and the bins have the same width. $E_{z(GW)}$ in D months presents a rising trend from 8 to 17 LT. After that time, it starts to decay. Close to 17 LT, it reaches its maximum value of around 1.5 mV/m. Also, $E_{z(GW)}$ in this season presents relatively high intensity

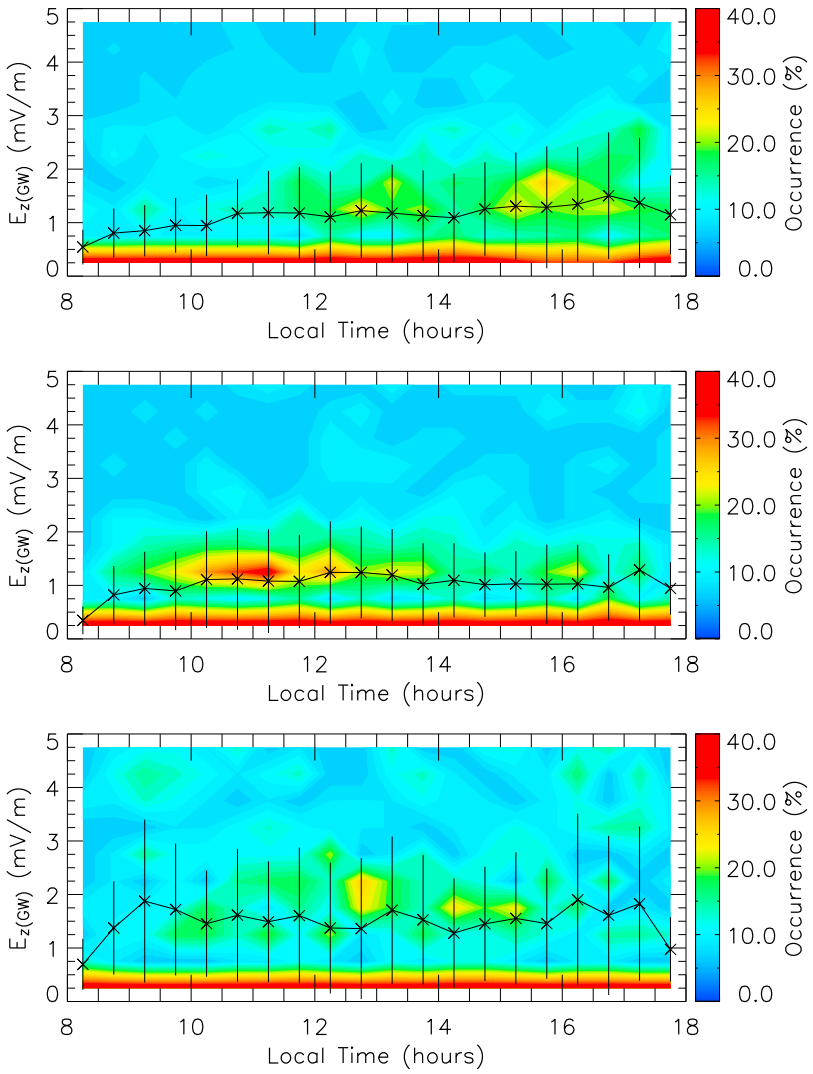

Figure 3. Statistics of occurrences of the $E_{z(GW)}$ amplitude as function of time for (top) solstice D months, (middle) equinoctial E months, and (bottom) solstice J months. The continuous line represents the average disturbed electric field for each 30-min interval, and the vertical line is the standard deviation of $E_{z(GW)}$.

(>1 mV/m) between 14 LT and 1730 LT. $E_{z(GW)}$ in E months starts with values close to zero and rise until 1.25 mV/m around midday. Indeed, it presents stronger values between ~10–14 LT. $E_{z(GW)}$ in J months shows high activity during almost all the diurnal period. It presents ~1.5 mV/m between 9 LT and 1730 LT. Therefore, it seems that in the Brazilian sector the GW activity dominates the morning period in equinox, close to sunset hours in summer, and is highly active during the whole day in winter.

[12] Figure 4 shows the statistics of R_{GW} binned in 30-min intervals and 0.05 for solstice D months (Figure 4, top), equinoctial E months (Figure 4, middle), and solstice J months (Figure 4, bottom). The vertical and horizontal lines have the same meaning as in Figures 2 and 3. The efficiency factor shows very similar features like those described in $E_{z(GW)}$ analysis: strong activity in morning time during equinox, close to sunset hours in summer, and strong activity during the whole day in winter. During summer, close to 17 LT, the electric fields generated by gravity waves represent 20% of the total vertical electric field. Indeed, the $E_{z(GW)}$ represents more than 15% of E_z during the time range between 15 LT and 1730 LT. During equinox, the oscillatory electric fields represent more than 15% of the total electric fields between 10 LT and 14 LT. The maximum GW effect is observed close to 11 LT, where the factor reaches up to 17%. The winter was the season with strongest efficiency for GW activity in electric field, but without a good pattern (relatively observed in other seasons), as indicated by the high standard deviations. The disturbed electric fields represent 20% of the total electric fields almost the whole day. The exception is the first and the last time bin. The maximum appears close to 9 LT, where R_{GW} reaches 30%.

3.2. Periodicities

[13] The GW induced electric field analysis was performed using Continuous Wavelet Transform because only the data with no gaps have been analyzed. For the periodicity analysis the Lomb-Scargle periodogram technique [*Lomb*, 1976; *Scargle*, 1982] was chosen due to its quality

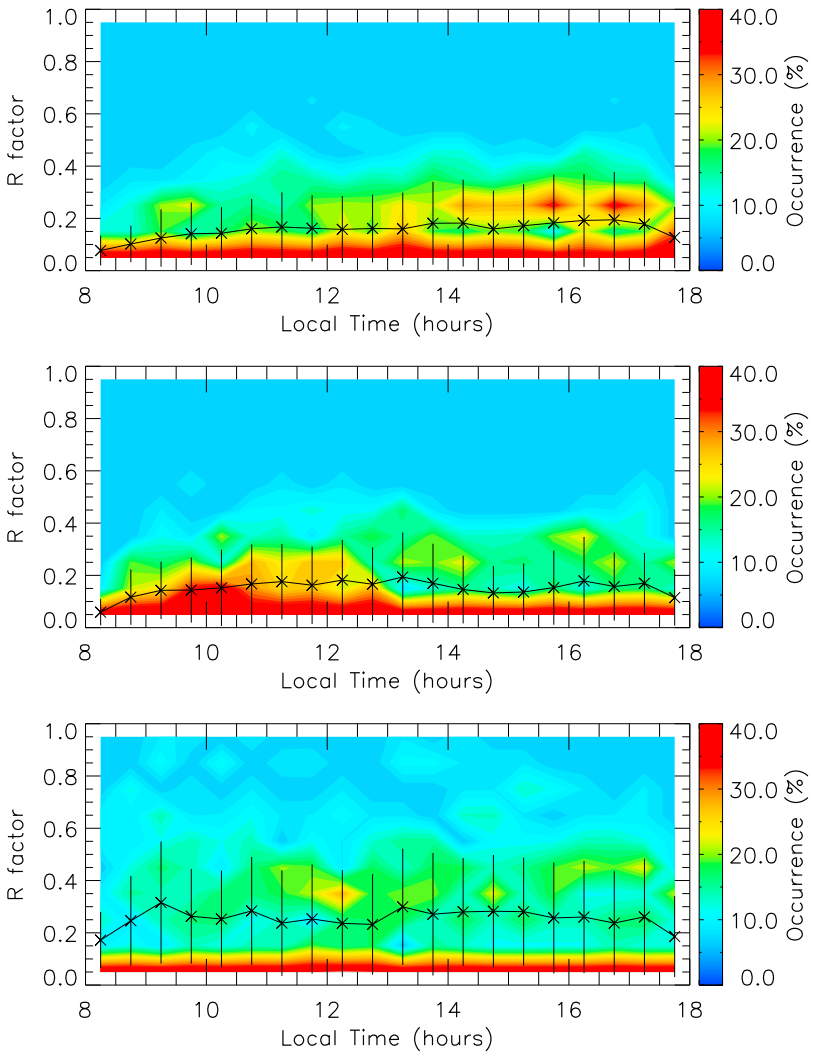

Figure 4. Statistics of occurrences of the R_{GW} as function of time for (top) solstice D months, (middle) equinoctial E months, and (bottom) solstice J months. The continuous line represents the average factor for each 30-min interval, and the vertical line is the standard deviation of R_{GW}.

of managing data gaps, since even the data sets having data gaps were included in the present analysis. The observed period which dominates the spectrum in the range from 4- to 30-min is extracted for each day. The histogram binned in 2-min interval for each season is shown in Figure 5. The overall characteristic is that the 4–6 min is the dominant bin, with the 6–8 min bin being the second dominant range period. Indeed, the 4–8 min periodicities concentrate almost 60% of the occurrences in any season. One remarkable feature is that during summer and equinox the 4–6 min bin is much higher than the others (>20%). During winter the difference between the 4–6 min and 6–8 min bins is less than 10%.

4. Discussion

4.1. Data Reliability

[14] In the present work the oscillations in the range from 4- to 30-min in the vertical electric field of the equatorial electrojet were analyzed. Based on previous theoretical studies by *Kato* [1973] and *Anandarao et al.* [1977], and on experimental studies by *Reddy and Devasia* [1976] and *Anandarao et al.* [1978], it may be assumed that all these short-term fluctuations are caused by gravity waves. Another possible source of short-term variations in the electric fields of the equatorial electrojet are disturbance electric fields due to magnetic storms, which have been discarded through the selection of magnetically quiet days only.

[15] It must be remembered that problems related to edge effect of the wavelet filtering were taken into account by removing results having data gaps or close to the edges from the analysis. Therefore, the data reliability is assured. Also, and more important, the results obtained for the time range close to sunset and sunrise (the edges of our data) do not include data having edge effects. However, the number of samples at this time range is reduced compared to other local times considered in the analysis.

[16] The observations between 1730 LT and 18 LT can be affected by the current reversal, which is caused by the zonal background electric field inversion. At this time the Type II irregularities disappear, so it is not possible to infer

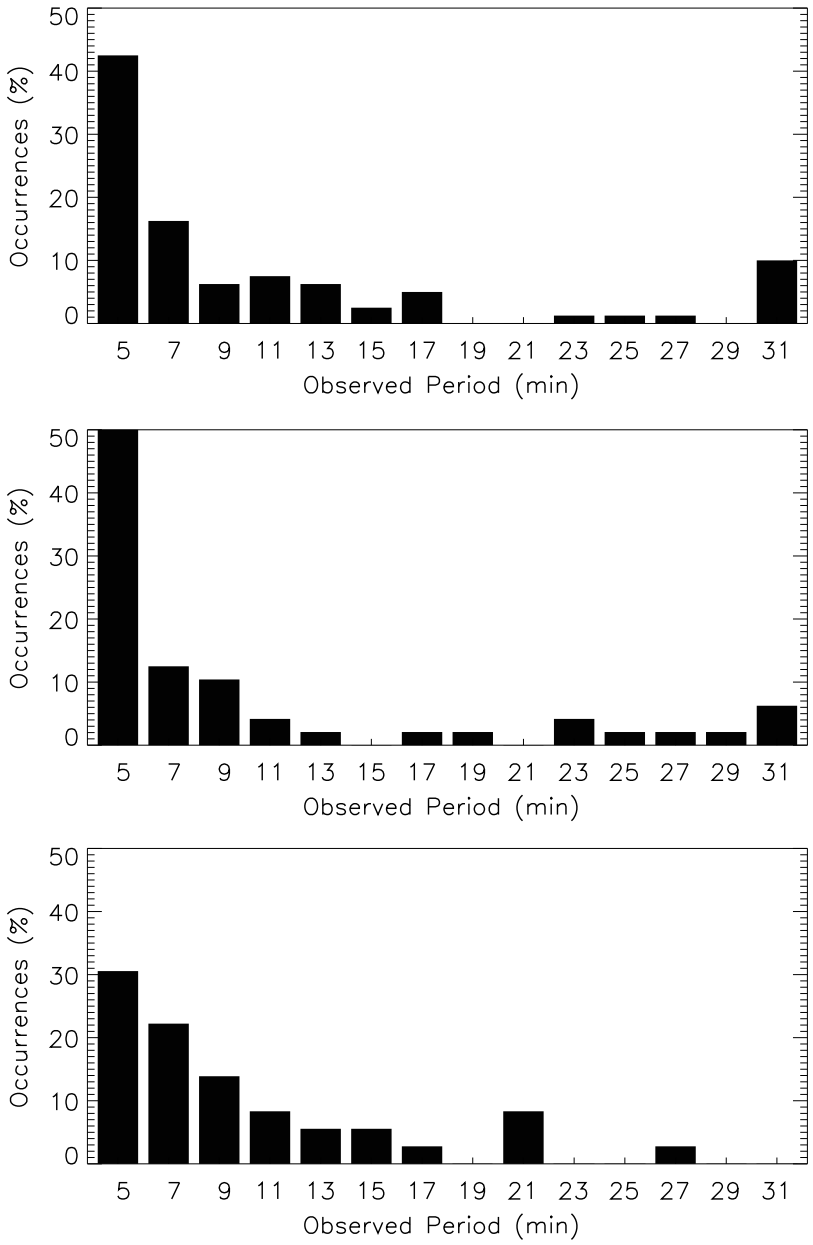

Figure 5. Histogram of the observed period binned in 2-min intervals for (top) D, (middle) E, and (bottom) J seasons.

gravity wave information, i.e., the GW activity could still be strong after that time (in the first nighttime hours).

4.2. Comparison With Previous Airglow Measurements

[17] Results of gravity wave observations using airglow measurements in the Brazilian equatorial sector at around 90 km height have been published by *Medeiros et al.* [2007] and *Taylor et al.* [1997]. These authors divide the GW observations in two groups: bands, that correspond to extensive, freely propagating (or ducted) gravity waves; and ripples, that are waves of a much smaller scale and transient nature. Since the current data analysis does not discriminate the GW types, the achieved results are a combination of both waves, and do not permit an identification of the dominant mode. Although, since the bulk observed by the radar beam is large, the radar should observe only the band types.

[18] *Taylor et al.* [1997] carried measurements over Alcantara, Brazil (2.3° S, 44.5° W), during the period August–October 1994 as part of the Guara campaign, a joint cooperative effort between National Aeronautics and Space Administration (NASA) and Instituto Nacional de Pesquisas Espaciais (INPE). Over 50 wave events were imaged by *Taylor et al.* [1997] from which a statistical study of the characteristics of equatorial gravity waves have been performed. *Medeiros et al.* [2007] carried airglow emission measurements at São João do Cariri (7° S, 36° W), from October 2000 to December 2004. A large amount of image data, more than 3000 h of observation and around 1000 wave events were analyzed.

Table 1. Gravity Wave Periodicities From Airglow Image Data Compared to the Current Results

	Taylor et al. [1997]		*Medeiros et al.* [2007]		Present Study
Parameter	Bands	Ripples	Bands	Ripples	(General)
Observed Mean Period (min)	9.6	5.1	11.1	9.6	10.4

[19] Combining our whole data set (2001, 2002, and 2004) in one single group and reanalyzing the observed periodicities (similar to what is done in Figure 5), the average periodicity for the whole period was calculated. A comparison among the present results, the results from *Taylor et al.* [1997], and the results from *Medeiros et al.* [2007] are summarized in Table 1. As mentioned before, GW types are not discriminated in the present work. However, a vis-à-vis comparison of the periodicities does not show any clear difference between results obtained in the present study and the band-like structures previously reported for the Brazilian equatorial sector. As far as we know there is no report about the difference of GW characteristics between daytime and nighttime, but since the atmospheric characteristics varies, some differences were expected. For instance, analyzing acoustic-gravity waves (AGW), *Antonova et al.* [2006] showed that there is a general shift of the spectrum of natural oscillations of the atmosphere toward the high-frequency (low-periodicity) region caused by solar radiation absorption and atmospheric emission of an equilibrium thermal radiation. Although, it is not necessarily the case that gravity waves must present the same behavior.

4.3. Overall Features and Implications

[20] The statistics of vertical electric field perturbations (related to gravity wave winds) show different behavior for different seasons. D months concentrate most of the GW occurrences in the hours close to sunset, between 15 LT and 17 LT. Most of the occurrences in the morning period are likely to be observed in the E months. Differently of the other two seasons, GW occurrences in J months are spread all over daytime. Despite of this remarkable differences, there is no report of seasonal variation effects in the coupling between the *E* and *F* regions related to this matter. The results that $E_{z(GW)}$ in summer are more probable to occur close to sunset may have some implications to *F* region also. The Spread *F* Experiment (SpreadFEx) was a campaign performed in late 2005 designed to define the potential role of neutral atmosphere dynamics, primarily gravity waves propagating upward from the lower atmosphere, in seeding equatorial spread *F* (ESF) and plasma bubbles extending to higher altitudes. The various analyses of neutral atmosphere and ionosphere dynamics and structure described in the "The Spread *F* Experiment (SpreadFEx): Coupling from the lower atmosphere to the ionosphere" special issue (*Annals of Geophysics*, 2008) provide evidence of gravity waves connection with plasma bubbles [*Fritts et al.*, 2008]. Hence, the strong gravity wave activity close to sunset in summer, when spread *F* occurrences in the Brazilian sector are higher [*Abdu et al.*, 1992], may indicate a connection between the events. Further investigation to identify cause-effect relationship need to be conducted, however.

[21] Gravity wave kinetic energy as well as variances in each of the three components of the wind direction have shown a semiannual variation at these altitudes with maxima in summer and winter and minima in spring and fall [*Fritts and Alexander*, 2003, and references therein]. The results of *Kovalam et al.* [2006] showed strong diurnal modulation of the GW wind velocities with peaks in the midmorning and close to sunset. Such modulation of the velocities is due to the effect of the diurnal tide, which has nonnegligible amplitudes in horizontal winds, even near the equator. Another effect that must be taken into account is the effect of tidal temperature perturbations, which are quite substantial at equatorial latitudes. A well-known effect is the modulation of the Brunt-Vaisalla frequency. From such results, changes in the vertical wavelength of gravity waves and hence the saturation conditions can be observed. The overall diurnal variability in the gravity wave winds is therefore a consequence of a complicated interaction between the tidally induced winds and temperature variability itself. So, the results of seasonal behavior obtained from the present work seem to be due to a combination of tidal modulation and semiannual variation.

[22] Finally, it should be mentioned that the methodology presented here has some limitations. It does not provide any information about the vertical or horizontal wavelengths (or wave number). Also, the polarization electric field generated by the gravity wave is $-\mathbf{U} \times \mathbf{B}$ ($-|U| \cdot |B| \cdot \sin\theta$), which means that the electric field oscillations are dependent of the angular relation between the direction of the wind oscillation and the Earth's magnetic field lines. If the wave propagates in a direction such that the winds oscillations are perpendicular to the magnetic field, the effect is maximized. If the declination of the radar site is close to 0°, it may be more suitable to infer features from the zonal component of the gravity wave such as zonal wavelength, zonal wave number, and zonal velocity and its variance. Since this study is based on radar data from São Luís Space Observatory (OESLZ), with ~20° of declination, the present results may have some small contributions from meridional component of the GW neutral winds.

5. Conclusions

[23] From the Type II EEJ irregularity velocities obtained from coherent backscatter radar measurements, some gravity wave characteristics were inferred and their influence in the vertical ionospheric electric fields were studied. A comparison between the electric field periodicity results from the present study and gravity wave periodicities in the equatorial South American sector based on airglow measurements showed good agreement. The vertical electric field perturbations related to gravity wave winds show a seasonal variation in their occurrences. The daytime higher GW activity in D months appears to occur close to sunset; in the morning hours, in E months; and with relatively higher GW activity almost in the whole daytime during J months. This seasonal behavior seems to result from combination of tidal modulation and semiannual variation. The high GW activity near sunset in summer, when spread *F* occurrences in the Brazilian sector are higher, may indicate some

connection between the phenomena. However, such effect needs to be further investigated to identify cause-effect relationship.

[24] **Acknowledgments.** The authors thank L. M. Guizelli, P. D. S. C. Almeida, and L. C. A. Resende for their help in radar data processing. One of the authors, H.C.A., thanks CNPq/MCT for financial support to his MSc program through the project 131326/2007-4.

[25] Amitava Bhattacharjee thanks the reviewers for their assistance in evaluating this paper.

References

Abdu, M. A., I. S. Batista, and J. H. A. Sobral (1992), A new aspect of magnetic declination control of equatorial spread *F* and *F* region dynamo, *J. Geophys. Res.*, *97*, 14,897–14,904.

Abdu, M. A., C. M. Denardini, J. H. A. Sobral, I. S. Batista, P. Muralikrishna, and E. R. de Paula (2002), Equatorial electrojet irregularities investigations using a 50 MHz back-scatter radar and a digisonde at São Luís: some initial results, *J. Atmos. Sol. Terr. Phys.*, *64*, 1425–1434.

Anandarao, B. G., R. Raghavarao, and C. R. Reddy (1977), Electric fields by gravity wave winds in the equatorial ionosphere, *J. Geophys. Res.*, *82*, 1510–1512.

Anandarao, B. G., R. Raghavarao, J. N. Desai, and G. Haerendel (1978), Vertical winds and turbulence over Thumba, *J. Atmos. Terr. Phys.*, *40*, 157–163.

Antonova, V. P., K. E. Dungenbaeva, A. V. Zalizovskii, A. S. Inchin, S. V. Kryukov, V. M. Somsikov, and Y. M. Yampol'skii (2006), Difference between the spectra of acoustic gravity waves in daytime and nighttime hours due to nonequilibrium effects in the atmosphere, *Geomagn. Aeron.*, *46*(1), 101–109.

Aveiro, H. C., C. M. Denardini, and M. A. Abdu (2009), Signatures of 2-day wave in the *E* region electric fields and their relationship to winds and ionospheric currents, *Ann. Geophys.*, *27*, 631–638.

Broche, P., M. Crochet, and J. Gagnepain (1978), Neutral winds and phase velocity of the instabilities in the equatorial electrojet, *J. Geophys. Res.*, *83*, 1145–1146.

Buneman, O. (1963), Excitation of field aligned sound waves by electron streams, *Phys. Rev. Lett.*, *10*(7), 285–287.

Denardini, C. M., M. A. Abdu, and J. H. A. Sobral (2004), VHF radar studies of the equatorial electrojet 3-m irregularities over São Luís: day-to-day variabilities under auroral activity and quiet conditions, *J. Atmos. Sol. Terr. Phys.*, *66*, 1603–1613.

Earle, G. D., and M. C. Kelley (1987), Spectral studies of the sources of ionospheric electric fields, *J. Geophys. Res.*, *92*(A1), 213–224.

Eleman, F. (1973), The geomagnetic field, in *Cosmical Geophysics*, edited by A. Egeland et al., pp. 45–62, Scand. Univ. Books, Oslo.

Farley, D. T. (1963), A plasma instability resulting in field aligned irregularities in the ionosphere, *J. Geophys. Res.*, *68*(A22), 6083–6097.

Fejer, B. G., and M. C. Kelley (1980), Ionospheric irregularities, *Rev. Geophys.*, *18*(2), 401–454.

Forbes, J. M. (1981), The equatorial electrojet, *Rev. Geophys.*, *19*(3), 469–504.

Fritts, D. C., and M. J. Alexander (2003), Gravity wave dynamics and effects in the middle atmosphere, *Rev. Geophys.*, *41*(1), 1003, doi:10.1029/2001RG000106.

Fritts, D. C., et al. (2008), Gravity wave and tidal influences on equatorial spread *F* based on observations during the Spread *F* Experiment (SpreadFEx), *Ann. Geophys.*, *26*, 3235–3252.

Kato, S. (1973), Electric field and wind motion at the magnetic equator, *J. Geophys. Res.*, *78*, 757–762.

Kovalam, S., R. A. Vincent, and P. Love (2006), Gravity waves in the equatorial MLT region, *J. Atmos. Sol. Terr. Phy.*, *68*, 266–282.

Lomb, N. R. (1976), Least-squares frequency analysis of unequally spaced data, *Astrophys. Space Sci.*, *39*, 447–462.

Medeiros, A. F., H. Takahashi, R. A. Buriti, J. Fechine, C. M. Wrasse, and D. Gobbi (2007), MLT gravity wave climatology in the South America equatorial region observed by airglow imager, *Ann. Geophys.*, *25*, 399–406.

Reddy, C. A., and C. V. Devasia (1976), Short period fluctuations of the equatorial electrojet, *Nature*, *261*, 396–397.

Rogister, A., and N. D'Angelo (1970), Type II irregularities in the equatorial electrojet, *J. Geophys. Res.*, *75*, 3879–3887.

Sato, T. (1975), Neutral winds and electrojet irregularities, *J. Geophys. Res.*, *80*(19), 2835–2838.

Scargle, J. D. (1982), Studies in astronomical time series analysis. II. Statistical aspects of spectral analysis of unevenly spaced data, *Astrophys. J.*, *263*, 835–853.

Taylor, M. J., W. R. Pendleton Jr., S. Clark, H. Takahashi, D. Gobbi, and R. A. Goldberg (1997), Image measurements of short-period gravity waves at equatorial latitudes, *J. Geophys. Res.*, *102*(D22), 26,283–26,299.

M. A. Abdu, H. C. Aveiro, and C. M. Denardini, Divisao de Aeronomia, Instituto Nacional de Pesquisas Espaciais, S. J. Campos, SP 12227-010, Brazil. (maabdu@dae.inpe.br; aveiro@dae.inpe.br; denardin@dae.inpe.br)